

Downregulation of *Dlx5* and *Dlx6* expression by *Hand2* is essential for initiation of tongue morphogenesis

Francie Barron¹, Crystal Woods¹, Katherine Kuhn¹, Jonathan Bishop¹, Marthe J. Howard² and David E. Clouthier^{1,†}

SUMMARY

Lower jaw development is a complex process in which multiple signaling cascades establish a proximal-distal organization. These cascades are regulated both spatially and temporally and are constantly refined through both induction of normal signals and inhibition of inappropriate signals. The connective tissue of the tongue arises from cranial neural crest cell-derived ectomesenchyme within the mandibular portion of the first pharyngeal arch and is likely to be impacted by this signaling. Although the developmental mechanisms behind later aspects of tongue development, including innervation and taste acquisition, have been elucidated, the early patterning signals driving ectomesenchyme into a tongue lineage are largely unknown. We show here that the basic helix-loop-helix transcription factor *Hand2* plays key roles in establishing the proximal-distal patterning of the mouse lower jaw, in part through establishing a negative-feedback loop in which *Hand2* represses *Dlx5* and *Dlx6* expression in the distal arch ectomesenchyme following *Dlx5*- and *Dlx6*-mediated induction of *Hand2* expression in the same region. Failure to repress distal *Dlx5* and *Dlx6* expression results in upregulation of *Runx2* expression in the mandibular arch and the subsequent formation of aberrant bone in the lower jaw along with proximal-distal duplications. In addition, there is an absence of lateral lingual swelling expansion, from which the tongue arises, resulting in aglossia. *Hand2* thus appears to establish a distal mandibular arch domain that is conducive for lower jaw development, including the initiation of tongue mesenchyme morphogenesis.

KEY WORDS: Aglossia, bHLH, Craniofacial, Hinge and caps, Homeosis, Neural crest cell, Mouse

INTRODUCTION

Most of the craniofacial skeleton arises from neural crest cells (NCCs), including the bone, cartilage and connective tissue of the face, neck and tongue (Hall, 1982). Arising along the neural folds of vertebrates before migrating ventrally into the pharyngeal arches (Bronner-Fraser, 1995; Couly et al., 1996; Kontges and Lumsden, 1996; Le Douarin, 1982), NCCs are patterned by numerous environmental cues (Chai and Maxson, 2006). These signals, organized into hierarchical cascades, initiate NCC patterning and differentiation, thus determining both their identity and fate (Clouthier and Schilling, 2004; Depew and Simpson, 2006).

In contrast to our knowledge of the signals regulating bone and cartilage development in the mandibular portion of the first pharyngeal arch, the early signals initiating tongue morphogenesis are poorly understood. Development of the tongue involves NCCs both from three pharyngeal arches and from somitic myoblasts (Noden and Francis-West, 2006). Although the mouse mandibular arch is a complex structure composed of multiple tissue and gene expression domains at embryonic day (E) 10.5 (Depew and Simpson, 2006; Clouthier and Schilling, 2004), a noticeable tongue bud is not evident. However, by E12.5, a recognizable tongue is present and includes somitic myoblasts that have migrated through the hypoglossal duct and that will give rise to the tongue

musculature (Noden and Francis-West, 2006). Besides transforming growth factor-beta receptor 2 (*Tgfr2*) signaling (Hosokawa et al., 2010), the identity of other factors regulating this early aspect of tongue morphogenesis is not known.

One key pathway responsible for establishing the proximal-distal organization of the pharyngeal arches is initiated by signaling from the endothelin-A receptor (*Ednra*) located on NCCs (Clouthier et al., 1998; Yanagisawa et al., 1998). *Ednra* signaling is induced soon after NCCs reach the pharyngeal arches by its ligand, endothelin-1 (*Edn1*) (Clouthier et al., 1998; Maemura et al., 1996; Miller et al., 2000; Yanagisawa et al., 1998). This initiates one or more signaling cascades responsible for NCC identity and fate within the mandibular pharyngeal arch (Clouthier et al., 2010; Clouthier and Schilling, 2004). Two induced factors, *Dlx5* and *Dlx6*, contribute to the ‘*Dlx* code’ hypothesized to establish proximal-distal identity within the arches (Depew et al., 2002; Depew and Simpson, 2006; Depew et al., 2005; Jeong et al., 2008). Loss of *Ednra*, *Edn1*, or *Dlx5* and *Dlx6* results in homeotic transformation of mandibular arch-derived bone and soft tissue structures into more maxillary-like derivatives (Beverdam et al., 2002; Depew et al., 2002; Ozeki et al., 2004; Ruest et al., 2004). However, aglossia is not observed in any mouse mutants in the *Ednra* pathway (*Ednra*, *Edn1*, *Ece1*, *Mef2c*, *Dlx5*, *Dlx6*) (Clouthier et al., 2010).

One direct transcriptional target of *Dlx5* and *Dlx6* is the gene encoding the basic helix-loop-helix transcription (bHLH) factor *Hand2* (Charité et al., 2001). Although *Hand2* mutant mice die by E10.5 owing to vascular defects (Thomas et al., 1998; Yamagishi et al., 2000), fate mapping *Hand2* daughter cells using the *Hand2* arch-specific enhancer (Charité et al., 2001) illustrated that these cells were found throughout most of the lower jaw (Ruest et al., 2003a). In addition, ventral arch cartilage derivatives in *hand2* mutant zebrafish (*han^{s6}*), which survive longer than mouse

¹Department of Craniofacial Biology, University of Colorado Anschutz Medical Campus, Aurora, CO 80045, USA. ²Department of Neuroscience, University of Toledo Health Sciences Center (formerly Medical College of Ohio before merger with the University of Toledo), Toledo, OH 43614, USA.

[†]Author for correspondence (david.clouthier@ucdenver.edu)

mutants), are severely affected (Miller et al., 2003) and early gene expression is disrupted. In mice, targeted deletion of the *Hand2* arch-specific enhancer (*Hand2^{BA/BA}*) results in only partial loss of the *Hand2* expression domain in the mandibular arch and limited developmental changes (Yanagisawa et al., 2003). However, NCC-specific deletion of *Hand1* (the other Hand gene expressed in the pharyngeal arches) (Clouthier et al., 2000; Cserjesi et al., 1995) on the hypomorphic *Hand2^{BA/BA}* background resulted in cleft palate and a small, thickened mandible (Funato et al., 2009). Based on in vitro findings, the changes in the mandible were hypothesized to result from a loss of Hand2-Runx2 interaction, leading to changes in bone ossification. However, the full function of Hand2 in facial morphogenesis is not clear, as *Hand2* was not completely inactivated in these mice.

To address problems associated with global *Hand2* inactivation, two groups have created *Hand2* conditional knockout mice. Conditional ablation of *Hand2* in NCCs has revealed a crucial role for Hand2 in the development of sympathetic ganglion neurons (Hendershot et al., 2008; Morikawa et al., 2007), the enteric nervous system (Hendershot et al., 2007; D'Autreaux et al., 2007) and the cardiac outflow tract (Holler et al., 2010). In addition, conditional inactivation of Hand2 in the developing palatal epithelium has uncovered a role for Hand2 in palatal shelf fusion (Xiong et al., 2009). However, the role of Hand2 in NCC patterning and differentiation during craniofacial development has yet to be examined. In this report, we show that inactivating *Hand2* specifically in NCCs leads to changes in jaw development, with the most striking being aglossia. These changes are preceded by an earlier failure to downregulate *Dlx5* and *Dlx6* expression in the distal mandibular arch, indicating that Hand2-mediated repression of *Dlx5* and *Dlx6* expression is crucial for establishing a domain in the mandibular arch that is conducive for tongue mesenchymal morphogenesis.

MATERIALS AND METHODS

Mice

Hand2^{flox/flox} (*Hand2^{fl/fl}*) (Hendershot et al., 2007; Hendershot et al., 2008), *Hand2^{fl/-}* (Hendershot et al., 2008), *Wnt1-Cre* (Danielian et al., 1998) and *R26R* (Soriano, 1999) mice have been described previously.

Breeding and genotyping

Hand2^{fl/fl} mice were bred with *Wnt1-Cre* transgenic mice to generate *Hand2^{fl/+}*; *Wnt1-Cre* animals. *Hand2^{fl/+}*; *Wnt1-Cre* mice were bred with *Hand2^{fl/fl}* mice to generate *Hand2^{fl/fl}*; *Wnt1-Cre* embryos (referred to as *Hand2^{cko}*). For fate-mapping experiments, *Hand2^{fl/fl}* mice were bred with *R26R* mice (Soriano, 1999) to homozygosity. These mice were then bred with *Hand2^{fl/+}*; *Wnt1-Cre* animals to create *Hand2^{fl/fl}*; *Wnt1-Cre*; *R26R^{+/+}* embryos. *Hand2^{fl}*, *Cre* and *lacZ* genotyping were performed as described previously (Ruest and Clouthier, 2009; Soriano, 1999; Hendershot et al., 2008).

Skeleton staining

Skeleton (Ruest and Clouthier, 2009) and cartilage (Clouthier et al., 1998) staining was performed as described previously. Stained bone and cartilage preparations were analyzed and photographed using an Olympus SZX12 stereomicroscope fitted with a DP11 digital camera.

Whole-mount β -galactosidase staining

β -galactosidase staining was performed as described previously (Ruest et al., 2003a).

Histology

For histological analysis, E18.5 embryos were fixed, embedded in paraffin, sectioned and stained as described previously (Ruest et al., 2004). For immunostaining, sections were incubated with monoclonal anti-skeletal myosin (1:400; MY-32; Sigma, St Louis, MO, USA), anti-TROMO-1

(1:25; Developmental Studies Hybridoma Bank, Iowa City, IA, USA), and/or Alexa Fluor 568 phalloidin (Invitrogen) as described previously (Clouthier et al., 1997). Trichrome staining was performed as described previously (Clouthier et al., 1997). After staining, all sections were examined and photographed with an Olympus BX50 compound microscope fitted with an Olympus DP71 digital camera.

In situ hybridization

Whole-mount in situ hybridization (ISH) analysis was performed as described previously (Clouthier et al., 1998) using digoxigenin (DIG)-labeled antisense cRNA riboprobes against *Dlx1*, *Dlx2*, *Dlx3*, *Dlx5*, *Dlx6*, *FoxF1* (*Foxf1a* – Mouse Genome Informatics), gooseoid homeobox (*Gsc* – Mouse Genome Informatics), *Hand1*, *Hand2*, *Msx1*, *Msx2*, *Pitx1*, *Pitx2*, *Runx2*, sonic hedgehog and *Twist1*. Embryos were photographed using an Olympus SZX12 microscope as described above.

Real-time PCR

Mandibular pharyngeal arches were collected and stored in RNA Later (Ambion) until genotyped. RNA was collected from arches using the QIAshredder and RNeasy kits (Qiagen). cDNA was prepared from total RNA using the Quantitect cDNA Synthesis Kit (Qiagen). Real-time quantitative PCR was performed using 5 ng of cDNA and the Quantitect SYBR Green PCR Kit (Qiagen), including Quantitect Assay primers (Qiagen). RT-PCR and data analysis was performed using a MyiQ2 machine (BioRad).

Volume measurements for the *Runx2* expression domain

Volume measurements for *Runx2* expression following ISH were conducted using ImageJ software (<http://rsb.info.nih.gov/ij/>) (Abramoff et al., 2004). Briefly, the scale (pixels/micron) was calculated using a micrometer and the ImageJ ruler tool, then was set globally in ImageJ. A region of interest (ROI) was specified using the polygon tool. The lower jaw ROI was specified as the entire lower jaw. We included the tongue in control embryos to ensure that our area measurements between control and *Hand2^{cko}* embryos were equivalent (as *Hand2^{cko}* embryos lack a tongue). The *Runx2* ROI was specified as the entire region exhibiting DIG reactivity. Once the ROIs were outlined, the total area contained in the outlined region was calculated in ImageJ using the Measure tool. The percentage of expression was calculated by dividing the *Runx2* ROI area by the lower jaw ROI area. Measurements were conducted on three embryos of each genotype and values averaged.

Analysis of cellular proliferation and apoptosis

Three 7 μ m sections through the rostral, middle and caudal aspects of the mandibular arch, each separated by 60 μ m, were used. Analysis of cell death at E10.5 was performed using the DeadEnd Labeling Kit (Promega) as described previously (Abe et al., 2007). Detection of cell death at E11.5 was performed using the In Situ Cell Death Detection Kit (Roche). Proliferating cells at both ages were detected using 5-ethynyl-2'-deoxyuridine (EdU) incorporation and the Invitrogen Click-It EdU Kit (Promega). At E10.5, these assays were conducted on consecutive sections; at E11.5, assays were performed on the same section. After staining, slides were counterstained with 4',6-diamidino-2-phenylindole dihydrochloride (DAPI; Sigma, 2.0 μ g/ml) for 10 minutes, washed and coverslipped using ProLong Gold Antifade Reagent (Invitrogen). Images were captured using the DP71 digital camera, with reconstruction of the entire arch region accomplished using TrakEM2, a component of Fiji (<http://pacific.mpi-cbg.de>). To quantify cell death and proliferation in specific arch regions, a grid was manually placed over the arch image using Adobe Photoshop. Vertical grid lines were placed on the midline and the outermost regions of the left and right lateral arch halves. The midline of the left or right arch half was then calculated by dividing the distance between lateral outer edge and arch midline in half; this established the boundary between the anterior/posterior arch and the lateral arch. Horizontal grid lines were calculated by setting the upper and lower limits at the point where the arch midline reaches the ectoderm. The length between upper and lower horizontal lines was then divided in two to create the horizontal midline of the arch, separating the anterior and posterior arch. Cell counts within the left and right lateral regions and posterior and anterior regions were then

manually counted using the Cell Counter plugin for ImageJ. The final incidence of proliferation and cell death was calculated as the number of proliferating or TUNEL-positive cells as a percentage of total cells.

Cell culture

MC3T3 cells (ATCC, Manassas, VA, USA) were maintained in MEM alpha (Invitrogen) supplemented with 20% fetal bovine serum (Sigma), penicillin/streptomycin (Invitrogen), and fungizone (Invitrogen) at 37°C in a humidified chamber with 5% CO₂.

Luciferase assays

MC3T3 cells seeded on 12-well plates were transfected with 0.05 µg pRL-TK (Promega), 0.5 µg pGL3-I56i-luc [generated by placing the I56i enhancer both 5' and 3' of the firefly luciferase cDNA in the pGL3 (Promega) vector] or pGL3-I56i^{ΔEbox}-luc [created using the QuikChange Lightning Site-Directed Mutagenesis Kit (Stratagene); primers 5'-CAAATTGGATGGCACTGAAGCTGGAGGCTTTGTTC-3' and 5'-GAACAAAGCCTCCAGCTTCAGTGCCATCCATTG-3' were used to change the putative E-box site CAGCTG to AAGCTG within the pGL2-I56i-luc template vector], and 0.8 µg of each expression vector using Eugene 6 (Roche). Expression vectors included: pCS2+MT-Dlx5, pCS2+MT-Hand2, pCS2+MT-Hand1 (gift from Hiromi Yanagisawa, University of Texas Southwestern Medical Center, Dallas, TX, USA) and pDNA3.1+MT-ΔN⁽¹⁻⁹⁰⁾-Hand2 (gift from Anthony Firulli, Indiana University School of Medicine, Indianapolis, IN, USA). Experiments were performed in triplicate and collected 24 hours after transfection. Lysate was prepared and firefly (experimental reporter) and renilla (normalizing reporter) luciferases were measured simultaneously using the Dual-Luciferase Reporter Assay System (Promega) and a Luminoskan Ascent 2.4 machine (Thermo Scientific). Activity of the experimental reporter was calculated by dividing the firefly luciferase value by the renilla luciferase value. Fold change was then calculated by dividing the expression vector activity by the empty expression vector (mock) activity.

Statistical analysis

All statistical analysis of results was performed using an unpaired two-tailed *t*-test with Prism software (GraphPad).

RESULTS

Changes in facial development in *Hand2*^{fl/fl}; *Wnt1*-Cre embryos

Mice homozygous for the conditional allele (*Hand2*^{fl/fl}) were viable, healthy and fertile (Hendershot et al., 2007; Hendershot et al., 2008) and showed no alterations in skull morphology (data not shown). We next crossed *Hand2*^{fl/fl} mice with the *Wnt1*-Cre transgenic strain to target the *Hand2* gene deletion to NCCs (Chai et al., 2000). Grossly, E18.5 *Hand2*^{fl/fl}; *Wnt1*-Cre (*Hand2*^{cko}) embryos had retrognathia and low-set pinnae (data not shown) along with mystacial vibrissae (the whisker-like sensory organs normally confined to the snout) on the lower jaw epithelium (data not shown).

Alizarin Red- and Alcian Blue-stained E18.5 *Hand2*^{cko} skeletons revealed a loss of both the angular processes of the mandible and the tympanic rings, significant retrognathia and an almost complete loss of Meckel's cartilage (Fig. 1B,D,H,J,L). Bone structures resembling duplicated pterygoid bones were fused to the actual pterygoid bones (Fig. 1F), indicating a role for *Hand2* in establishing or maintaining NCC identity. Also, in contrast to *Hand2*^{BA/BA} embryos (Barbosa et al., 2007; Funato et al., 2009; Yanagisawa et al., 2003), gross cleft palate was not observed (Fig. 1F), indicating that *Hand2* does not play a direct role in NCC-mediated palatal shelf elevation. In the lower jaw, the mandible was dysmorphic, resembling the mandible seen in *Hand2*^{BA/BA}; *Hand1*^{fl/fl}; *Wnt1*-Cre embryos (Barbosa et al., 2007; Funato et al., 2009). A second bilateral membranous bone ran medial to the mandible (asterisks in Fig. 1H,J), though its identity was not clear. Other changes included aberrantly ossified body and lesser horns of the hyoid bone, with the latter fused, either

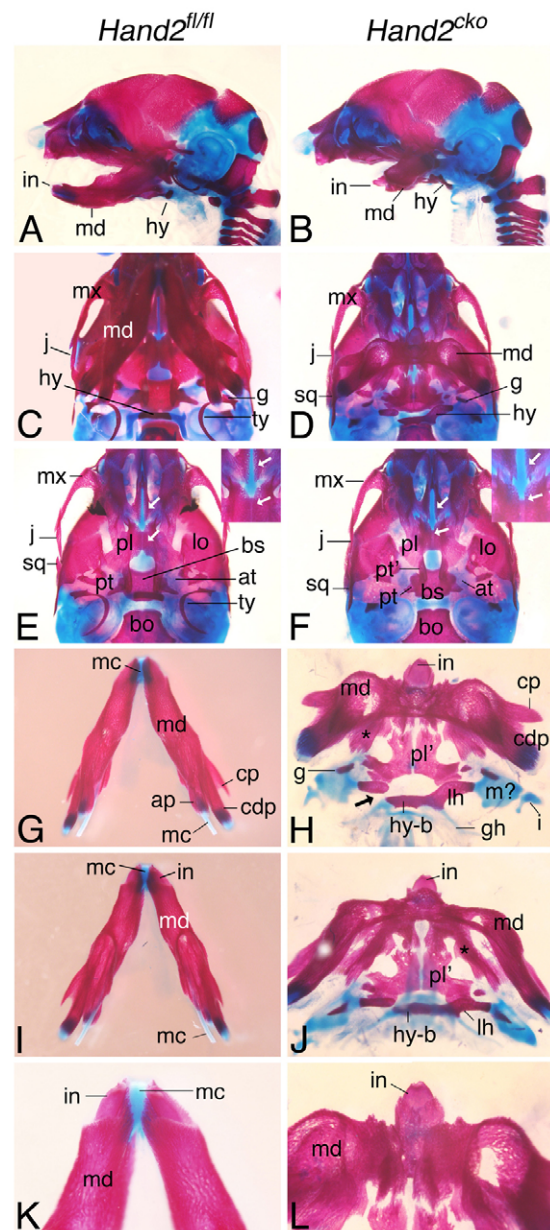


Fig. 1. Analysis of *Hand2*^{cko} embryo skulls. Alizarin Red (bone) and Alcian Blue (cartilage)-stained E18.5 *Hand2*^{fl/fl} (left column) and *Hand2*^{cko} (right column) mouse embryos. (A,B) Lateral view illustrates retrognathia. (C-F) Ventral view shows loss of tympanic rings (ty), absence of cleft palate (white arrows, magnified in insets) and duplicated pterygoid bones (pt') in *Hand2*^{cko} embryos (D,F). (G,H) Ventral view of the *Hand2*^{cko} mandible complex shows duplicated palatine bones (pl'), loss of the angular processes (ap) of the mandible (md) and Meckel's cartilage (mc), and unilateral fusion of the hyoid bone to middle ear cartilage (H). (I,J) Oral view of a *Hand2*^{cko} mandible shows the presence of aberrant bone medial to the mandible (asterisks in H,J). (K,L) Incisors (in) in *Hand2*^{cko} embryos are fused. at, ala temporalis; bo, basioccipital; bs, basisphenoid; cdp, condylar process; cp, coronoid process; g, gonial; gh, greater horns of the hyoid; hy, hyoid; hy-b, body of hyoid; i, incus; j, jugal; lh, lesser horns of the hyoid; lo, lamina obturans; mx, maxilla; sq, squamosal.

unilaterally or bilaterally, to duplicated palatine bones (Fig. 1H,J). In addition, both lesser horns also formed articulations with the malformed cartilage anlage of the mallei (Fig. 1H,J; data not shown),

whereas the greater horns articulated with the styloid process (data not shown). Finally, only a single midline incisor was observed in most embryos (Fig. 1H,J,L), though two closely abutting lower incisors were also observed in some embryos (data not shown). Because skull defects in E18.5 *Hand2^{fl/fl};Wnt1-Cre* embryos were identical to those observed in *Hand2^{fl/fl};Wnt1-Cre* embryos (data not shown), the remainder of our analysis was performed using *Hand2^{fl/fl};Wnt1-Cre* embryos. Taken together, these changes suggest that *Hand2* plays crucial roles in both NCC patterning and establishment of NCC identity in the mandibular arch.

Histological analysis of skull structures reveals aglossia

In serial frontal sections through the head of E18.5 control and *Hand2^{cko}* embryos, aberrant bone was observed running along the medial mandible (Fig. 2B). Only a single incisor was present along the midline, whereas upper and lower molar development appeared normal (Fig. 2B; data not shown). Mystacial vibrissae on the lower jaw epithelium were also observed (Fig. 2D), and rugae, raised epithelial ridges normally confined to the roof of the mouth, were duplicated on the lower oral cavity surface (Fig. 2D). That duplicated vibrissae and rugae were also observed in *Edn1*, *Ednra* and *Dlx5/Dlx6* mutant embryos (Depew et al., 2002; Ozeki et al., 2004; Ruest et al., 2004) suggest that loss of *Hand2* might contribute to these mandibular to maxillary transformations.

The most striking finding in *Hand2^{cko}* embryos was the absence of a tongue (Fig. 2B,D,F,H,L). In frontal and sagittal sections, a cleft existed where the tongue should normally reside, though a small amount of muscle was present at the cleft base (asterisk in Fig. 2D; m in Fig. 2H,J). Although the tongue was absent, the tongue epithelium was present. In both control and *Hand2^{cko}* embryos, the delineation between the non-keratinized and keratinized stratified squamous epithelium of tongue was readily apparent (red arrows in Fig. 2A,B; black arrows in Fig. 2F). Squamous cells overlying the keratinized epithelium were also present in control and *Hand2^{cko}* embryos, though fewer were observed in *Hand2^{cko}* embryos (Fig. 2E-H). We also identified taste buds in both control (Fig. 2I) and *Hand2^{cko}* (Fig. 2J) embryos using an antibody against cytokeratin-8 (CK8, Troma-1; Krt8 – Mouse Genome Informatics), a taste bud marker (Thirumangalathu et al., 2009). Taken together, our results indicate that although a failure of NCC patterning, proliferation or differentiation leads to a near absence of tongue mesenchyme, partial tongue epithelial development occurs.

Tongue morphogenesis requires the interaction of NCC-derived cells and myoblasts (Hosokawa et al., 2010). Aglossia could, therefore, result from failed somitic myoblast migration to the future tongue domain. However, the muscle below the tongue of *Hand2^{cko}* embryos was stained by phalloidin (an F-actin marker) (Fig. 2J). Similarly, anti-myosin staining was observed in the anterior lower jaw of *Hand2^{cko}* embryos (white arrow in Fig. 2L), though it was far more scattered than that observed in control embryos (Fig. 2K). Thus, although we cannot rule out a partial myoblast migration defect, the aglossia does not appear to be due to a complete absence of myoblasts.

Tongue mesenchyme morphogenesis is never initiated

We next examined gross oral morphology in control and *Hand2^{cko}* embryos between E12.5 and E13.5. As a marker, we used sonic hedgehog (*Shh*) expression, which is expressed by the incisor buds, palatal rugae and developing taste papilla of the tongue. At E12.5,

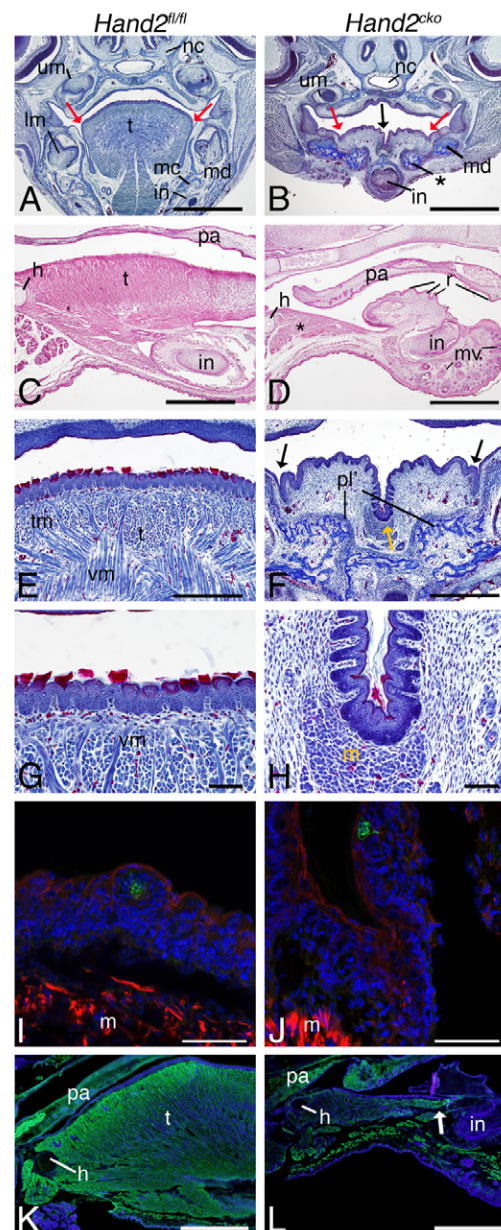


Fig. 2. Histological analysis of *Hand2^{cko}* embryo skulls. Frontal (A,B,E-I) and sagittal (C,D,K,L) sections from E18.5 *Hand2^{fl/fl}* (left column) and *Hand2^{cko}* (right column) mouse embryos. (A,B) Trichrome-stained sections show the mandible (md), aberrant bone (asterisk) and absent tongue (t; black arrow in B). Red arrows distinguish the junction between non-keratinized and keratinized stratified squamous epithelium. (C,D) Hematoxylin and eosin-stained sagittal sections illustrate aglossia, limited muscle (asterisk), rugae (r) in the upper and lower oral ectoderm and mystacial vibrissae (mv) on the lower jaw ectoderm (D). (E-H) Trichrome staining illustrates the non-keratinized to keratinized stratified squamous epithelium transition (black arrows in F) and the presence of keratin (red) in both control (E,G) and mutant (F,H) tongue epithelium. Limited muscle is present in the mutants (yellow arrow in F; m in H). (I,J) Immunofluorescent staining [nuclei, blue (DAPI); F-actin, red (phalloidin); immature taste buds, green (cytokeratin-8)] detects taste buds in the tongue epithelium in both control and mutant embryos. (K,L) Using an anti-myosin antibody (green), muscle is detected in the anterior oral cavity (white arrow). Counterstained with DAPI. h, hyoid; in, incisor; mc, Meckel's cartilage; nc, nasal capsule; pa, palate; pl, palatine bones; tm, transversus muscle; vm, verticalis muscle; lm, lower molars; um, upper molars.

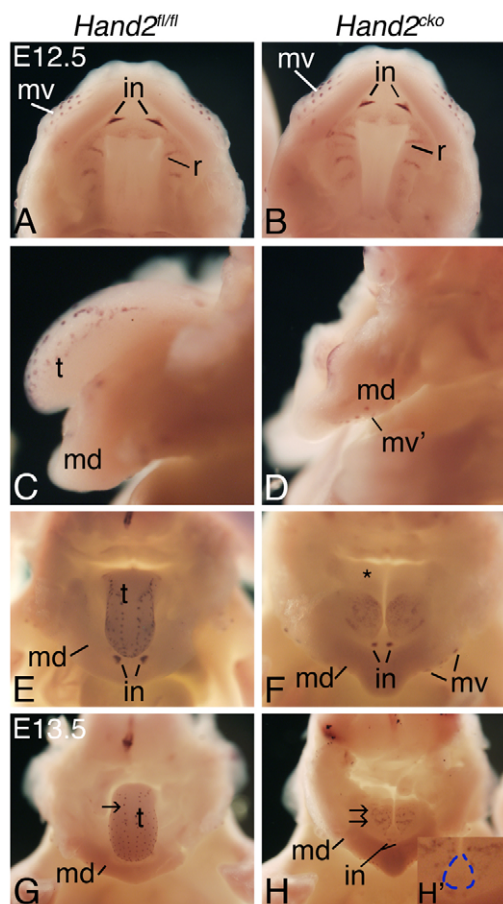


Fig. 3. Tongue development of *Hand2*^{cko} embryos. *Shh* expression in *Hand2*^{fl/fl} (left column) and *Hand2*^{cko} (right column) mouse embryos. (A,B) Oral view of the upper jaw from E12.5 control and *Hand2*^{cko} embryos shows *Shh* expression in developing mystacial vibrissae (mv), incisors (in) and rugae (r). (C-F) In E12.5 control embryos, *Shh* expression is observed in the fungiform papilla of the tongue (t) (C,E). With the tongue absent (asterisk) in *Hand2*^{cko} embryos, expression is observed diffusely in the anterior oral cavity (F) and in aberrant mystacial vibrissae (mv') (D). (G-H') At E13.5, *Shh* expression in the lower jaw of controls remains in fungiform papilla (arrow in G), whereas expression in the anterior oral cavity in *Hand2*^{cko} embryos has organized into horizontal stripes resembling rugae of the upper jaw (arrows in H). The aberrant proximal-distal seam has persisted in the lower jaw and joined two other seams in the anterior oral cavity that resemble the fusion point of the primary and secondary palates in the upper jaw (see blue lines in H'). md, mandible.

Shh expression in the upper jaw of control and *Hand2*^{cko} embryos was observed in the mystacial vibrissae, palatal rugae and incisor fields (Fig. 3A,B). In the lower jaw of control embryos, *Shh* expression was observed in the incisor domains and fungiform papilla on the tongue (Fig. 3C,E). By contrast, although *Shh* expression in E12.5 *Hand2*^{cko} embryos marked the incisor fields, expression was also observed in the anterior soft tissue and aberrant mystacial vibrissae (Fig. 3D,F), but was absent in the posterior soft tissue, consistent with absence of tongue development (asterisk in Fig. 3F). By E13.5, *Shh* expression in control embryos was still observed in the fungiform papilla (Fig. 3G). In E13.5 *Hand2*^{cko} embryos, *Shh* expression in the lower jaw had resolved into lateral lines that resembled developing palatal rugae (black arrows in Fig.

3H). Although a midline cleft was still present, it met two other clefts anteriorly that together formed the appearance of primary and secondary palates (see lines in Fig. 3H'). The primary and secondary palates are complex structures; not all aspects of these structures were duplicated in the lower jaw of *Hand2*^{cko} embryos. However, it does appear that loss of *Hand2* disrupts tongue morphogenesis and leads to partial transformation of NCC fate from a mandibular to maxillary identity.

Changes in proliferation and cell death in *Hand2*^{cko} embryos

Aglossia could result from defects in NCC or somitic myoblast migration to the pharyngeal arches, or their subsequent proliferation and survival. Because *Hand2* expression within the ectomesenchyme is first observed at ~E9.25-9.5 (Clouthier et al., 2000; Thomas et al., 1998), NCC migration defects were not expected (Abe et al., 2007; Chai et al., 2000). To confirm this, we crossed the *Hand2* conditional mutant strain into the *R26R* Cre reporter strain (Soriano, 1999) and found that in E10.5 embryos, the distribution of β -gal-labeled cells was similar in the arches of both *Hand2*^{fl/+}; *R26R*; *Wnt1-Cre* and *Hand2*^{cko}; *R26R*; *Wnt1-Cre* embryos (data not shown). This indicates that NCC migration was unaffected by loss of *Hand2*.

Conventional targeting of *Hand2* in mice results in widespread mandibular arch mesenchyme apoptosis by E10.0 (Thomas et al., 1998). Thus, we examined changes in both cellular proliferation and apoptosis in E10.5 and E11.5 control and *Hand2*^{cko} mandibular arches using a grid pattern that would allow us to determine if and where (lateral, anterior or posterior) changes were occurring (Fig. 4A). Because the tongue arises from the posterior arch, changes in this region could provide a partial mechanism for the observed aglossia. We found that the percentage of proliferating cells was similar between control and *Hand2*^{cko} embryos at E10.5 in the lateral and posterior arch (Fig. 4B). However, in the anterior arch, EdU incorporation was slightly but significantly elevated. By E11.5, proliferation was statistically similar in control and *Hand2*^{cko} embryos throughout the mandibular arch (Fig. 4B). Examination of cell death using TUNEL revealed a significant increase in apoptotic nuclei in the lateral mandibular arch of both E10.5 and E11.5 *Hand2*^{cko} embryos compared with that observed in control embryos (Fig. 4C). Although the incidence of apoptosis trended higher in the posterior arch domain of E11.5 *Hand2*^{cko} embryos, the change was not statistically significant. These data indicate that decreased proliferation and increased cell death are not major contributors to the observed aglossia.

Gene expression analysis of *Hand2*^{cko} embryos

To define the molecular changes that accompany the observed cellular changes, we performed whole-mount ISH analysis on E10.5 control and *Hand2*^{cko} embryos. As expected, *Hand2* expression was absent in the pharyngeal arches of *Hand2*^{cko} embryos (Fig. 5B). Surprisingly, expression of *Hand1* was almost completely downregulated in the mandibular arch (Fig. 5D). This suggests that *Hand1* expression in this area is under transcriptional control of another signaling pathway. *Gsc*, a gene involved in mouse middle ear development (Rivera-Perez et al., 1995; Yamada et al., 1995), is downregulated in the pharyngeal arches of *han*^{sc6} zebrafish (Miller et al., 2003), a pattern also observed in the pharyngeal arches of *Hand2*^{cko} embryos (Fig. 5F). By contrast, the zebrafish *msx* genes *msxb* and *msxe* are upregulated in the pharyngeal arches of *han*^{sc6} embryos (Miller et al., 2003). However, we found that the expression

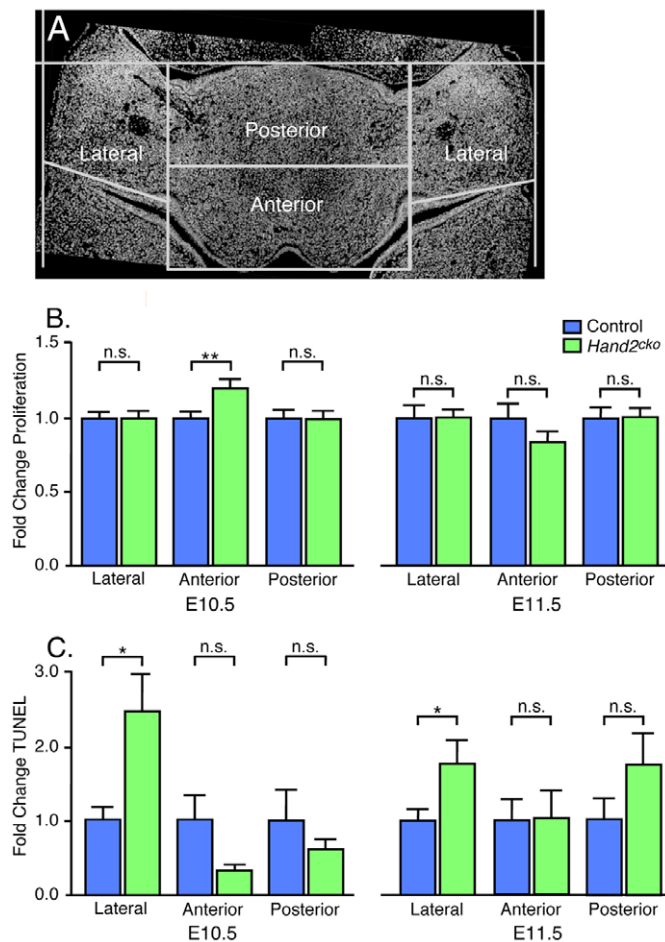


Fig. 4. Cell proliferation and death in *Hand2^{cko}* mouse embryo arches. (A) A representative section showing the grid used for analysis of proliferation and cell death. (B,C) Sections from EdU-treated embryos were analyzed for EdU incorporation (proliferation, B) and TUNEL (apoptosis, C). After counterstaining with DAPI, labeled and total cells were manually counted. The percentage of labeled cells was calculated as the total number of EdU- or TUNEL-positive cells divided by the total number of DAPI positive cells, with this number then used to calculate fold change from control. Error bars represent s.e.m. * $P < 0.05$; ** $P < 0.01$; n.s., not significant ($P > 0.05$). All other significance numbers are at least $P > 0.1$ except for the change in anterior arch TUNEL between E10.5 control and *Hand2^{cko}* embryos ($P = 0.07$).

of *Msx1* and *Msx2* was unchanged in *Hand2^{cko}* embryos (Fig. 5L,N), as were *Pitx1* and *Pitx2* (Fig. 5P,R), both involved in lower jaw and incisor development (Gage et al., 1999; Lin et al., 1999; Liu et al., 2003; Mitsiadis and Drouin, 2008). Expression of *Twist1* was also examined, as it can interact with *Hand2* to influence limb development (Firulli et al., 2005; McFadden et al., 2002) and shows an expanded expression domain that parallels the decreased *Hand2* expression domain in *Ednra^{-/-}* embryos (Ruest et al., 2004). However, *Twist1* expression in *Hand2^{cko}* embryos did not appear grossly different (Fig. 5T). Expression of the distal-less gene family members *Dlx2* and *Dlx3* was also not noticeably changed (Fig. 5H,J). Finally, *FoxF1* expression was examined, as it appears to be involved in distal lower jaw morphogenesis downstream of *Shh* (Jeong et al., 2004). However, *FoxF1* expression was unchanged in *Hand2^{cko}* embryos (Fig. 5V).

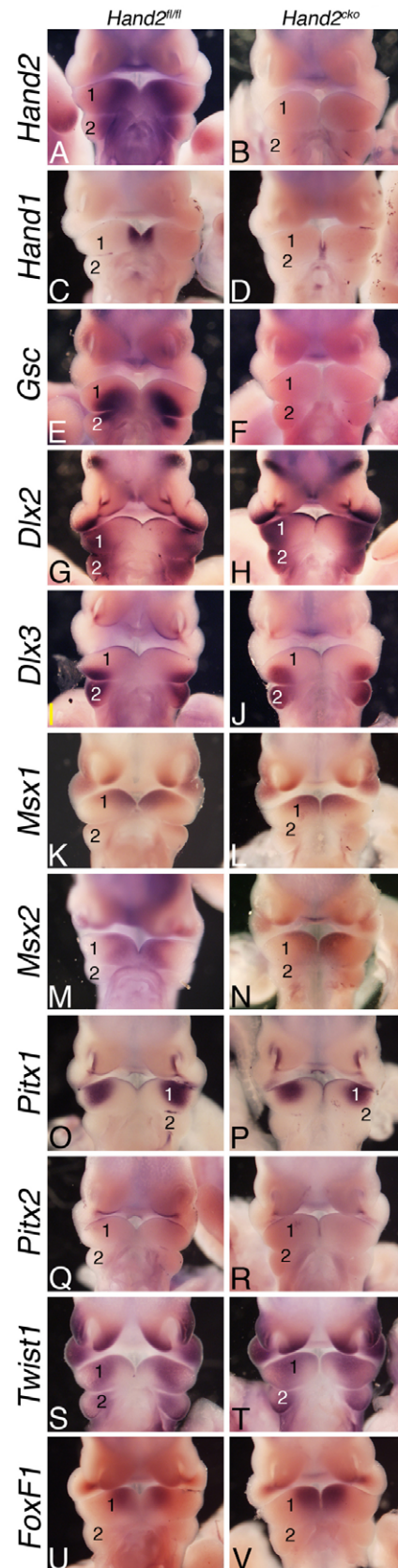


Fig. 5. Gene expression analysis in *Hand2^{cko}* embryos. (A-V) In situ hybridization analysis of the indicated genes in E10.5 *Hand2^{fl/fl}* (left column) and *Hand2^{cko}* (right column) mouse embryos. 1, mandibular pharyngeal arch; 2, second pharyngeal arch.

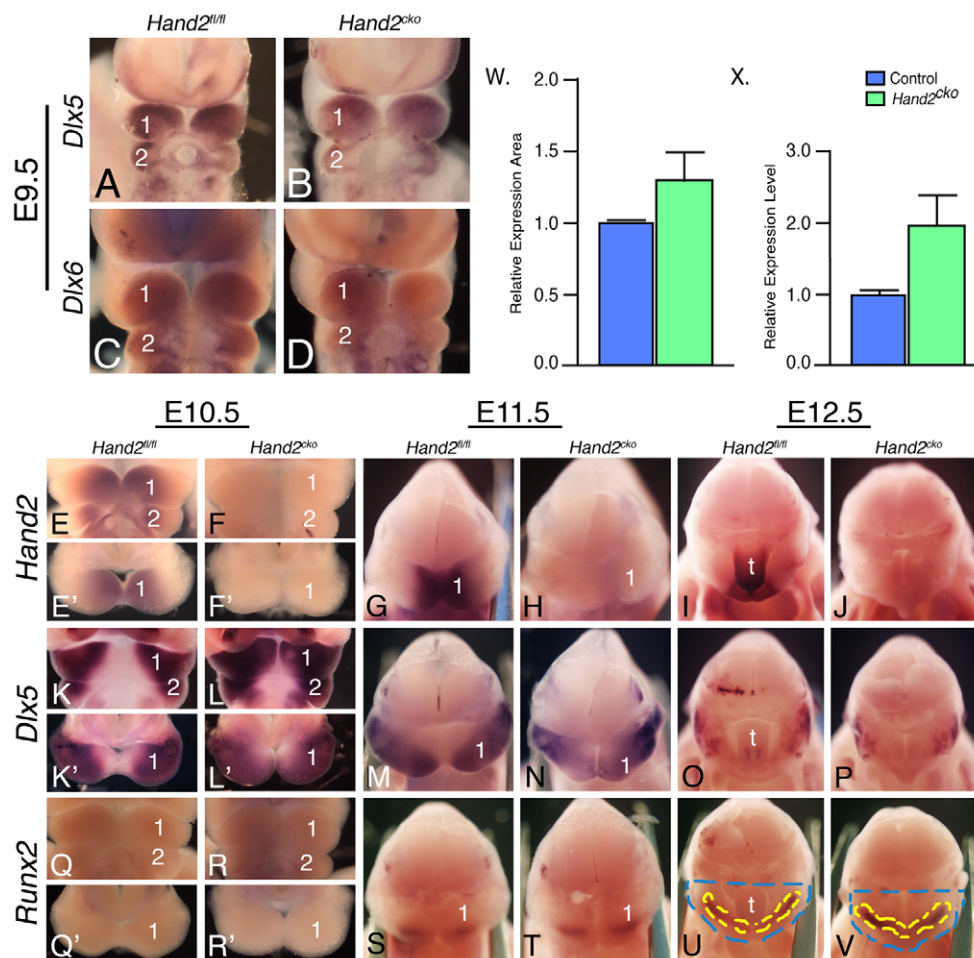


Fig. 6. *Hand2*, *Dlx5* and *Runx2* expression analysis in *Hand2*^{cko} embryo arches. (A–V) In situ hybridization analysis of *Dlx5* (A,B,K–P), *Dlx6* (C,D), *Hand2* (E–J) and *Runx2* (Q–V) expression in E9.5–12.5 *Hand2*^{fl/fl} (left column of each time point) and *Hand2*^{cko} (right column of each time point) mouse embryos. (A–D) Ventral views of *Dlx5* (A,B) and *Dlx6* (C,D) expression in E9.5 embryos. (E–F') Ventral (E,F) and oral (E',F') views of *Hand2* expression. (G–J) An oral view of *Hand2* expression in the mandibular arch at both E11.5 (G,H) and E12.5 (I,J). (K–L') Ventral (K,L) and oral (K',L') views of *Dlx5* expression at E10.5. (M–P) Oral views of *Dlx5* expression in the mandibular arch at E11.5 (M,N) and E12.5 (O,P). (Q–R') Ventral (Q,R) and oral (Q',R') views of *Runx2* expression at E10.5. (S–V) Oral views of *Runx2* expression at E11.5 (S,T) and E12.5 (U,V). The area of the arch (blue dashed lines) and *Runx2* expression domains (yellow dashed lines) used for the calculation of *Runx2* expansion in Fig. 6W are denoted. (W) Quantification of *Runx2* expression area in E12.5 control and *Hand2*^{cko} embryos. Values are expressed relative to control values. (X) Analysis of *Runx2* expression in E12.5 mandibular arches. Levels were normalized against β -actin and expressed as fold change versus control levels. Error bars represent s.e.m.

Loss of *Hand2* leads to aberrant maintenance of both *Dlx5* and *Dlx6* expression

We also examined the expression of *Dlx5* and *Dlx6*, two genes that induce arch expression of *Hand2* (Charité et al., 2001; Depew et al., 1999; Depew et al., 2002). In E9.5 *Hand2*^{cko} embryos, *Hand2* expression was absent (data not shown), whereas *Dlx5* and *Dlx6* were both expressed throughout the mandibular arch of control and *Hand2*^{cko} embryos (Fig. 6A–D). By E10.5, *Hand2* expression in control embryos was observed in the disto-oral mandibular arch mesenchyme (Fig. 6E,E'), but was absent in *Hand2*^{cko} embryos (Fig. 6F,F'). *Dlx5* expression in E10.5 control embryos was downregulated in the distal and oral aspects of the mandibular arch but remained in the proximal arch (Fig. 6K,K'). By contrast, *Dlx5* expression was present throughout the mandibular arch of E10.5 *Hand2*^{cko} embryos (Fig. 6L,L'). By E11.5, *Hand2* message was present on the disto-oral surface of the mandibular arch in control embryos corresponding to the lateral lingual swelling (Fig. 6G). As observed in E10.5 control embryos, this coincided with a repression of *Dlx5* expression in the lateral lingual swelling (Fig. 6M). In E11.5 *Hand2*^{cko} embryos, *Hand2* expression was absent (Fig. 6H), with *Dlx5* expression continuing in the disto-oral region (Fig. 6N). By E12.5, *Hand2* expression in control embryos was confined to the tongue and distal mandibular arch (Fig. 6I), whereas *Dlx5* expression was confined to the tongue and proximal jaw (Fig. 6O). In E12.5 *Hand2*^{cko} embryos, *Hand2* expression was absent (Fig. 6J) whereas *Dlx5*, owing to the absence of the tongue, was only observed in the proximal jaw (Fig. 6P). The expression

pattern of *Dlx6* in control and *Hand2*^{cko} embryos was identical to that of *Dlx5* (data not shown). These results suggest that one function of *Hand2* is to restrict the expression domains of *Dlx5* and *Dlx6* from the distal mandibular arch.

Expression of *Dlx5* and *Dlx6* is an early event in osteogenesis and acts in part to induce *Runx2* expression (Holleuille et al., 2007), which is required for normal osteogenesis (Ducy et al., 1997; Komori et al., 1997; Otto et al., 1997). As *Hand2* can bind *Runx2* in vitro (Funato et al., 2009), we examined whether aberrant *Dlx5* and *Dlx6* expression in *Hand2*^{cko} embryos affected *Runx2* expression. At E10.5, *Runx2* expression was not detectable by ISH in control (Fig. 6Q,Q') or *Hand2*^{cko} (Fig. 6R,R') embryos. Likewise, *Runx2* expression was similarly present in the mandibular arches of E11.5 control and *Hand2*^{cko} embryos (Fig. 6S,T). However, by E12.5, *Runx2* expression in *Hand2*^{cko} embryos appeared expanded (Fig. 6V). These observations were supported by qRT-PCR, which showed an almost twofold increase in *Runx2* expression (Fig. 6X), and by area analysis (Fig. 6W). These results indicate that *Hand2* loss might lead to expanded initiation of an osteogenic pathway in the mandibular arch.

Hand2 represses *Dlx5* and *Dlx6* expression through the *Dlx5/Dlx6* pharyngeal arch-specific enhancer

To examine how *Hand2* might repress *Dlx5* and *Dlx6* expression, we transfected MC3T3-E1 cells with a luciferase reporter construct under control of the arch-specific intergenic enhancer from the

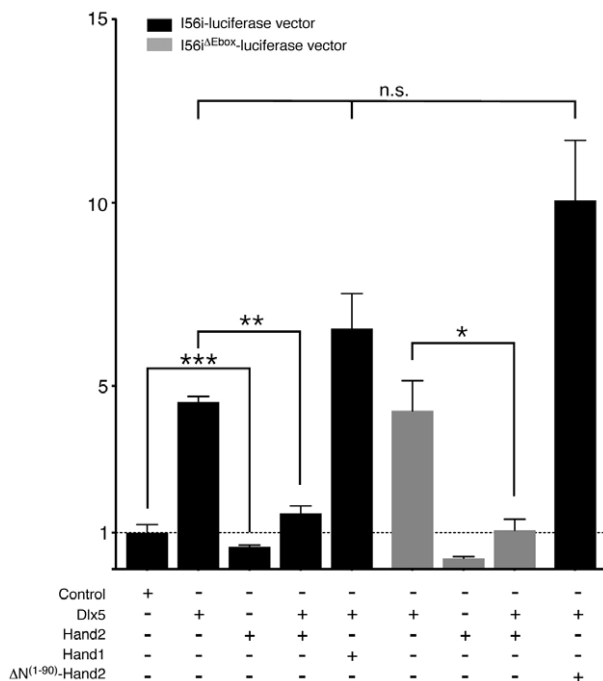


Fig. 7. In vitro analysis of *Hand2* repression of the *Dlx5/6* arch specific enhancer. An I56i-firefly luciferase vector was transfected into MC3T3-E1 cells along with other cDNAs and a renilla reporter construct (efficiency control). All conditions were normalized to corresponding empty vectors of gene expression constructs. Error bars represent s.e.m. Control, representative empty vector; *** $P < 0.0005$; ** $P < 0.005$; * $P < 0.05$; n.s., not significant ($P > 0.1$).

Dlx5/Dlx6 locus (Zerucha et al., 2000a). This enhancer, referred to as I56i, directs transgene expression to the *Dlx5/Dlx6* expression domain within the mandibular arch (Ruest et al., 2003b; Zerucha et al., 2000a). Co-transfection of the I56i-luciferase vector and *Dlx5*, a known inducer of the I56i enhancer, resulted in an almost fivefold increase in luciferase activity (Fig. 7). By contrast, co-transfection of the I56i-luciferase vector and *Hand2* led to a twofold reduction in luciferase activity (Fig. 7). Transfecting the I56i-luciferase vector with both *Dlx5* and *Hand2* resulted in essentially baseline levels of luciferase activity (Fig. 7), indicating that *Hand2* acts as a transcriptional repressor of *Dlx5* and *Dlx6* expression, with this repression being dominant to the activation effect of *Dlx5*. Similar results were obtained when *Dlx6* was used in place of *Dlx5* (data not shown). By contrast, co-transfection of the I56i-luciferase vector with *Dlx5* and *Hand1* did not block the inductive effect of *Dlx5*, illustrating that the effect is specific to *Hand2*.

As part of a bHLH dimer pair, *Hand2* binds to the E-box CANNTG and regulates transcription (Dai and Cserjesi, 2002). We examined the I56i enhancer for E-boxes and found one putative site in the 3' end of the enhancer. However, when the first nucleotide of this E-box was mutated from a C to an A (a mutation that should inactivate the E-box) (McLellan et al., 2006), the ability of *Hand2* to repress both basal enhancer activity and *Dlx5*-mediated activity was unchanged (Fig. 7), suggesting that *Hand2* was not acting through this E-box to regulate I56i activity. As *Hand2* has been previously demonstrated to interact with *Runx2* in vitro through *Hand2*'s N-terminal domain (Funato et al., 2009), we tested the ability of a mutant version of *Hand2* lacking the first

90 amino acids ($\Delta N^{(1-90)}$ -*Hand2*) to inhibit *Dlx5*-induced enhancer activity. In these experiments, $\Delta N^{(1-90)}$ -*Hand2* was unable to block *Dlx5*-induced luciferase activity, suggesting that *Hand2*'s N-terminal domain is crucial to *Hand2*'s ability to repress *Dlx5* and *Dlx6* expression. Although *Dlx5* does not appear to directly associate with *Hand2* (data not shown), *Hand2* could still act as part of a protein complex. Overall, our data indicates that *Hand2* is acting as a transcriptional repressor of *Dlx5* and *Dlx6* in the distal mandibular arch.

DISCUSSION

Although a 'Dlx code' appears to establish the proximal-distal identity of the mandibular arch during craniofacial development (for a review, see Depew and Simpson, 2006), the mechanism by which they act remains only partially elucidated. Here, we have shown that *Hand2* temporally limits the action of *Dlx5* and *Dlx6* during mandibular arch patterning. Loss of this negative-feedback loop leads to aglossia and loss of identity of the mandibular soft tissue. These findings illustrate that *Hand2* is likely to be a key mediator of the Dlx code during arch patterning.

Hand2 regulates mandibular arch patterning through negative regulation of *Dlx5* and *Dlx6*

Dlx5 and *Dlx6* induce *Hand2* expression in the distal half of the mandibular arch (Charité et al., 2001). Here, we have shown that *Hand2* then acts in a negative-feedback loop to shut down *Dlx5* and *Dlx6* expression in the *Hand2* domain, acting through the *Dlx5* and *Dlx6* intergenic arch-specific enhancer (Fig. 8). Although it might be surprising that changes limited to this distal domain can cause such extensive changes in lower jaw development, we have shown through analysis of *Hand2* daughter cell fate that the *Hand2* domain contributes to the entire lower jaw and much of the middle ear (excluding the incus and stapes) (Ruest et al., 2003a). Further, Bronner-Fraser and colleagues have illustrated in axolotl that the distal half of the mandibular arch gives rise to the lower jaw (mandible) whereas the proximal portion of the mandibular arch gives rise to more proximal hinge structures of the jaw (the palatoquadrate) (Cerny et al., 2004).

So why does the maintained presence of *Dlx5* and *Dlx6* lead to aglossia? Targeted disruption of *smoothed* (*Smo* – Mouse Genome Informatics) in the mandibular arch mesenchyme leads to loss of distal arch tissue and subsequent absence of the tongue and most of the lower jaw (Jeong et al., 2004). However, in these mutants, the expression of *Fox* genes, including *FoxF1*, was disrupted in the mandibular arch, accompanied by increased *Hand2* expression and distal arch cell death. Such changes were not observed in *Hand2*^{cko} embryos. Based on these findings, it does not appear that aglossia is due to absence of sufficient arch tissue. Rather, it would seem more likely that the distal arch tissue is repatterned owing to the presence of aberrant signals that include *Dlx5* and *Dlx6*, with this disrupting normal developmental interactions with other cell types, including somitic myoblasts. That some tongue muscle is present in near-term embryos probably reflects the complex signaling environment required for proper tongue muscle morphogenesis (Noden and Francis-West, 2006).

The findings from this study support the 'hinge and caps' model of jaw development (for a review, see Depew and Simpson, 2006). This model proposes that the polarity and modularity of the upper and lower jaws is driven by the articulation of the first arch prominences (the hinge) and signals located on the distal aspects of the two prominences and from the lamboid junction (where the maxillary prominence meets the olfactory placode) (the caps). Our

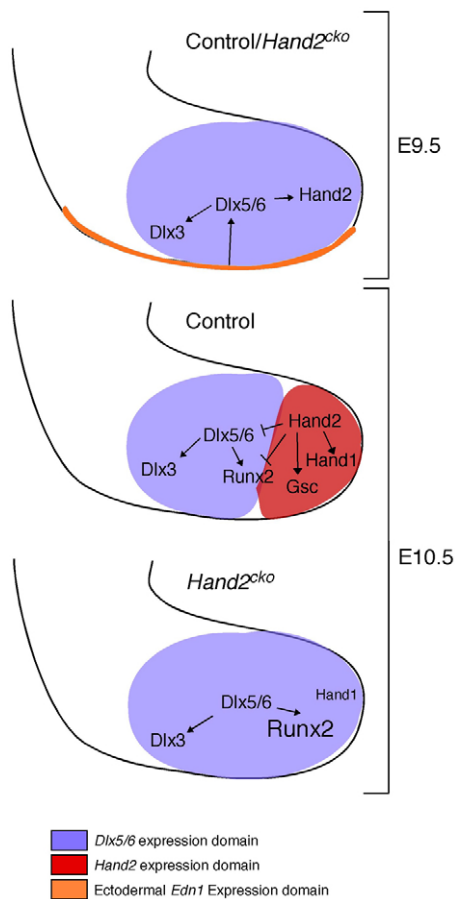


Fig. 8. Model of *Hand2* activation and regulation of *Dlx5* and *Dlx6* during mandibular arch development. At E9.5, ectodermal-derived Edn1 activates Ednra signaling in neural crest cells (NCCs), thus inducing *Dlx5* and *Dlx6* expression broadly within the mandibular arch. *Dlx5* and *Dlx6* in turn activate *Hand2* expression distally and *Dlx3* expression proximally. In E10.5 control animals, *Dlx5* and *Dlx6* expression is restricted from the distal arch by *Hand2*, which also activates or maintains expression of *Hand1* and *Gsc*. In *Hand2*^{cko} embryos, absence of *Hand2* leads to continued *Dlx5* and *Dlx6* expression in the distal arch and aberrant expression of *Runx2*. In addition, *Gsc* expression is lost and *Hand1* expression is greatly reduced.

findings support this model by illustrating that the loss of a cap signal (*Hand2*) specifically expressed in the distal mandibular arch mesenchyme disrupts jaw polarity (duplication of maxillary elements in the lower jaw). Further, our findings illustrate the importance of modular signals within the lower jaw, as improper regulation of cap signals (in this case, the failure to downregulate *Dlx5* and *Dlx6* expression in the distal arch) probably contributes to the observed *Hand2*^{cko} phenotype in the jaw, including changes in distal jaw shape and fused incisors. It will be important to understand better the communication between *Hand2* and the hinge region and to elucidate the molecules through which such communication occurs.

Hand2 function is crucial for osteogenic fates

Mouse embryos hypomorphic for *Hand2* have premature ossification of mandibular arch tissue (Barbosa et al., 2007; Funato et al., 2009). Based on both in vitro and in vivo data, Yanagisawa and colleagues proposed that *Hand2* could both repress early

Runx2 expression and antagonize *Runx2* activity via physical association and subsequent sequestration (Funato et al., 2009). Because *Runx2* is required for both the maintenance and differentiation of preosteoblastic mesenchyme into osteoblasts and subsequent initiation of osteogenesis (Bialek et al., 2004; Flores et al., 2006; Goldring et al., 2006; Hinoi et al., 2006), loss of either of these functions could lead to premature ossification and thus mandibular hypoplasia. Here, we show a third potential mechanism in which *Hand2* functions in a negative-feedback loop to inhibit distal *Dlx5* and *Dlx6* expression. As *Dlx5* can induce *Runx2* (Holleville et al., 2007; Miyama et al., 1999), failure to downregulate *Dlx5* and *Dlx6* expression in the distal arch mesenchyme would probably lead to enhanced *Runx2* expression (as shown in the present study) and thus the premature establishment of signaling cascades favorable to bone formation. Enhanced *Runx2* expression could also pattern neighboring cells that were competent to respond to *Runx2* but do not normally see it and could explain the presence of the aberrant bone in the lower jaw of our *Hand2*^{cko} embryos. It remains to be seen whether *Runx2* binds *Hand2* in vivo (Abe et al., 2009), though our model could allow aberrant *Runx2* activity without a physical interaction.

Hand gene dosage and bHLH dimer pools

As findings from this and other studies emerge illustrating the importance of *Hand* family members in developmental processes, one aspect to consider is whether both *Hand1* and *Hand2* have unique or redundant functions. A neural crest-specific deletion of *Hand1* on a hypomorphic *Hand2* background leads to jaw defects (Barbosa et al., 2007; Funato et al., 2009), suggesting that *Hand* proteins act redundantly in far distal arch development (i.e. in the *Hand2* domain in which *Hand1* is expressed). However, it is not possible to prove this point specifically, as we showed that *Hand2* regulates *Hand1* expression in the arch. The converse (that loss of *Hand1* in the NCC leads to loss of *Hand2*) is not true (Barbosa et al., 2007). One intriguing question to be addressed is whether the small amount of *Hand1* remaining in the distal arch is functionally significant. Answering this will require NCC-specific deletion of both *Hand1* and *Hand2*.

Another aspect to consider is how bHLH dimer pools change in response to loss of specific bHLHs within a cell. Although bHLHs can bind other factors through their 5' end (Bialek et al., 2004; Funato et al., 2009), they typically form dimer pairs with the ubiquitous class A bHLH molecules (such as E-proteins) or other class B bHLH proteins (Cai and Jabs, 2005; Firulli, 2003). When one dimer partner is removed, the stoichiometry of dimer pools is disrupted, allowing for potential changes in binding partners and subsequent aberrant gene regulation (Cai and Jabs, 2005). Dimer partner choice is known to influence strongly the cellular response to Twist family proteins (Firulli et al., 2003), with changes in Twist1-*Hand2* dimerization resulting in Saethre-Chotzen syndrome (Firulli et al., 2005). In addition, conditional disruption of either *Hand2* (this study) or *Twist1* (Rinon et al., 2007) in NCCs results in defects in craniofacial bone and cartilage structures. To understand fully the role of *Hand2* in facial morphogenesis, it will therefore be important to understand how loss of *Hand2* affects the function of other Twist family members, including Twist1.

Note added in proof

While this manuscript was in review, Talbot et al. (Talbot et al., 2010) reported that the expression of several *Dlx* genes expands into the ventral arches of *hand2* mutant zebrafish embryos.

Acknowledgements

We thank Nicholas Bennetts and Alicia Navetta for technical help and Hiromi Yanagisawa, Andrew McMahon and James Martin for probes. This work was supported by NIH grants DE018899 (to D.E.C.) and NS040644 and DK067064 (to M.J.H.). Deposited in PMC for release after 12 months.

Competing interests statement

The authors declare no competing financial interests.

References

- Abe, M., Ruest, L.-B. and Clouthier, D. E. (2007). Fate of cranial neural crest cells during craniofacial development in endothelin-A receptor deficient mice. *Int. J. Dev. Biol.* **51**, 97-105.
- Abe, M., Michikami, I., Fukushi, T., Abe, A., Maeda, Y., Ooshima, T. and Wakisaka, S. (2009). Hand2 regulates chondrogenesis *in vitro* and *in vivo*. *Bone* **46**, 1359-1368.
- Abramoff, M. D., Magelbaes, P. J. and Ram, S. J. (2004). Image Processing with ImageJ. *Biophotonics Int.* **11**, 36-42.
- Barbosa, A. C., Funato, N., Chapman, S., McKee, M. D., Richardson, J. A., Olson, E. N. and Yanagisawa, H. (2007). Hand transcription factors cooperatively regulate development of the distal midline mesenchyme. *Dev. Biol.* **310**, 154-168.
- Beverdam, A., Merlo, G. R., Paleari, L., Mantero, S., Genova, F., Barbieri, O., Janvier, P. and Levi, G. (2002). Jaw transformation with gain of symmetry after *Dlx5/Dlx 6* inactivation: mirror of the past. *Genesis* **34**, 221-227.
- Bialek, P., Kern, B., Yang, X., Schrock, M., Sosic, D., Hong, N., Wu, H., Yu, K., Ornitz, D. M., Olson, E. N. et al. (2004). A twist code determines the onset of osteoblast differentiation. *Dev. Cell* **6**, 423-435.
- Bronner-Fraser, M. (1995). Origins and developmental potential of the neural crest. *Exp. Cell Res.* **218**, 405-417.
- Cai, J. and Jabs, E. W. (2005). A twisted hand: bHLH protein phosphorylation and dimerization regulate limb development. *BioEssays* **27**, 1102-1106.
- Cerny, R., Lwigale, P., Ericsson, R., Meulemans, D., Epperlein, H.-H. and Bronner-Fraser, M. (2004). Developmental origins and evolution of jaws: new interpretations of "maxillary" and "mandibular". *Dev. Biol.* **276**, 225-236.
- Chai, Y. and Maxson, J. R. E. (2006). Recent advances in craniofacial morphogenesis. *Dev. Dyn.* **235**, 2353-2375.
- Chai, Y., Jiang, X., Ito, Y., Bringas, P., Jr, Han, J., Rowitch, D. H., Soriano, P., McMahon, A. P. and Sucov, H. M. (2000). Fate of the mammalian cranial neural crest during tooth and mandibular morphogenesis. *Development* **127**, 1671-1679.
- Charité, J., McFadden, D. G., Merlo, G. R., Levi, G., Clouthier, D. E., Yanagisawa, M., Richardson, J. A. and Olson, E. N. (2001). Role of *Dlx6* in regulation of an endothelin-1-dependent, *dHAND* branchial arch enhancer. *Genes Dev.* **15**, 3039-3049.
- Clouthier, D. E. and Schilling, T. F. (2004). Understanding endothelin-1 function during craniofacial development in the mouse and zebrafish. *Birth Defects Res. C* **72**, 190-199.
- Clouthier, D. E., Comerford, S. A. and Hammer, R. E. (1997). Hepatic fibrosis, glomerulosclerosis, and a lipodystrophy-like syndrome in *PEPCK-TGF-β1* transgenic mice. *J. Clin. Invest.* **100**, 2697-2713.
- Clouthier, D. E., Hosoda, K., Richardson, J. A., Williams, S. C., Yanagisawa, H., Kuwaki, T., Kumada, M., Hammer, R. E. and Yanagisawa, M. (1998). Cranial and cardiac neural crest defects in endothelin-A receptor-deficient mice. *Development* **125**, 813-824.
- Clouthier, D. E., Williams, S. C., Yanagisawa, H., Wieduwilt, M., Richardson, J. A. and Yanagisawa, M. (2000). Signaling pathways crucial for craniofacial development revealed by endothelin-A receptor-deficient mice. *Dev. Biol.* **217**, 10-24.
- Clouthier, D. E., Garcia, E. and Schilling, T. F. (2010). Regulation of facial morphogenesis by endothelin signaling: insights from mouse and fish. *Am. J. Med. Genet. A* **152**, 2962-2973.
- Couly, G. F., Grapin-Botton, A., Coltey, P. and Le Douarin, N. M. (1996). The regeneration of the cephalic neural crest, a problem revisited: the regenerating cells originate from the contralateral or from the anterior and posterior neural fold. *Development* **122**, 3393-3407.
- Cserjesi, P., Brown, D., Lyons, G. E. and Olson, E. N. (1995). Expression of the novel basic helix-loop-helix gene *eHAND* in neural crest derivatives and extraembryonic membranes during mouse development. *Dev. Biol.* **170**, 664-678.
- D'Autreaux, F., Morikawa, Y., Cserjesi, P. and Gershon, M. D. (2007). Hand2 is necessary for terminal differentiation of enteric neurons from crest-derived precursors but not for their migration into the gut or for formation of glia. *Development* **134**, 2237-2249.
- Dai, Y. S. and Cserjesi, P. (2002). The basic helix-loop-helix factor, HAND2, functions as a transcriptional activator by binding to E-boxes as a heterodimer. *J. Biol. Chem.* **277**, 12604-12612.
- Danielian, P. S., Muccino, D., Rowitch, D. H., Michael, S. K. and McMahon, A. P. (1998). Modification of gene activity in mouse embryos *in utero* by a tamoxifen-inducible form of Cre recombinase. *Curr. Biol.* **8**, 1323-1326.
- Depew, M. J. and Simpson, C. A. (2006). 21st century neonatology and the comparative development of the vertebrate skull. *Dev. Dyn.* **235**, 1256-1291.
- Depew, M. J., Liu, J. K., Long, J. E., Presley, R., Meneses, J. J., Pedersen, R. A. and Rubenstein, J. L. (1999). *Dlx5* regulates regional development of the branchial arches and sensory capsules. *Development* **126**, 3831-3846.
- Depew, M. J., Lufkin, T. and Rubenstein, J. L. (2002). Specification of jaw subdivisions by *Dlx* genes. *Science* **298**, 381-385.
- Depew, M. J., Simpson, C. A., Morasso, M. and Rubenstein, J. L. R. (2005). Reassessing the *Dlx* code: the genetic regulation of branchial arch skeletal pattern and development. *J. Anat.* **207**, 501-561.
- Ducy, P., Zhang, R., Geoffroy, V., Ridall, A. L. and Karsenty, G. (1997). *Osf2/Cbfa1*: a transcriptional activator of osteoblast differentiation. *Cell* **89**, 747-754.
- Fiurilli, A. B. (2003). A HANDful of questions: the molecular biology of the heart and neural crest derivatives (HAND)-subclass of basic helix-loop-helix transcription factors. *Gene* **312**, 27-40.
- Fiurilli, B. A., Howard, M. J., McDaid, J. R., McIlreavey, L., Dionne, K. M., Centonze, V. E., Cserjesi, P., Virshup, D. M. and Fiurilli, A. B. (2003). PKA, PKC, and the protein phosphatase 2A influence HAND factor function: a mechanism for tissue-specific transcriptional regulation. *Mol. Cell* **12**, 1225-1237.
- Fiurilli, B. A., Krawchuk, D., Centonze, V. E., Vargesson, N., Virshup, D. M., Conway, S. J., Cserjesi, P., Laufer, E. and Fiurilli, A. B. (2005). Altered Twist1 and Hand2 dimerization is associated with Saethre-Chotzen syndrome and limb abnormalities. *Nat. Genet.* **37**, 373-381.
- Flores, M. V., Lam, E. Y., Crosier, P. and Crosier, K. (2006). A hierarchy of Runx transcription factors modulate the onset of chondrogenesis in craniofacial endochondral bones in zebrafish. *Dev. Dyn.* **235**, 3166-3176.
- Funato, N., Chapman, S. L., McKee, M. D., Funato, H., Moriss, J. A., Shelton, J. M., Richardson, J. A. and Yanagisawa, H. (2009). Hand2 controls osteoblast differentiation in the branchial arch by inhibiting DNA binding of Runx2. *Development* **136**, 615-625.
- Gage, P. J., Suh, H. and Camper, S. A. (1999). Dosage requirement of *Pitx2* for development of multiple organs. *Development* **126**, 4643-4651.
- Goldring, M. B., Tsuchimochi, K. and Ijiri, K. (2006). The control of chondrogenesis. *J. Cell. Biochem.* **97**, 33-44.
- Hall, B. K. (1982). Mandibular morphogenesis and craniofacial malformations. *J. Craniofac. Genet. Dev. Biol.* **2**, 309-322.
- Hendershot, T. J., Liu, H., Sarkar, A. A., Giovannucci, D. R., Clouthier, D. E., Abe, M. and Howard, M. J. (2007). Expression of Hand2 is sufficient for neurogenesis and cell type-specific gene expression in the enteric nervous system. *Dev. Dyn.* **236**, 93-105.
- Hendershot, T. J., Liu, H., Clouthier, D. E., Shepherd, I. T., Coppola, E., Studer, M., Fiurilli, A. B., Pittman, D. L. and Howard, M. J. (2008). Conditional deletion of *Hand2* reveals critical functions in neurogenesis and cell type-specific gene expression for development of neural crest-derived noradrenergic sympathetic ganglion neurons. *Dev. Biol.* **319**, 179-191.
- Hinoi, E., Bialek, P., Chen, Y.-T., Rached, M.-T., Groner, Y., Behringer, R. R., Ornitz, D. M. and Karsenty, G. (2006). Runx2 inhibits chondrocyte proliferation and hypertrophy through its expression in the perichondrium. *Genes Dev.* **20**, 2937-2942.
- Holler, K. L., Hendershot, T. J., Troy, S. E., Vincentz, J. W., Fiurilli, A. B. and Howard, M. J. (2010). Targeted deletion of *Hand2* in cardiac neural crest-derived cells influences cardiac gene expression and outflow tract development. *Dev. Biol.* **341**, 291-304.
- Holleville, N., Mateos, S., Bontoux, M., Bollerot, K. and Monsoro-Burq, A.-H. (2007). *Dlx5* drives Runx2 expression and osteogenic differentiation in developing cranial suture mesenchyme. *Dev. Biol.* **304**, 860-874.
- Hosokawa, R., Oka, K., Yamaza, T., Iwata, J., Urata, M., Xu, X., Bringas, P., Jr, Nonaka, K. and Chai, Y. (2010). TGF-β mediated FGF10 signaling in cranial neural crest cells controls development of myogenic progenitor cells through tissue-tissue interactions during tongue morphogenesis. *Dev. Biol.* **341**, 186-195.
- Jeong, J., Mao, J., Tenzen, T., Kottmann, A. H. and McMahon, A. P. (2004). Hedgehog signaling in the neural crest cells regulates the patterning and growth of facial primordia. *Genes Dev.* **18**, 937-951.
- Jeong, J., Li, X., McEvilly, R. J., Rosenfeld, M. G., Lufkin, T. and Rubenstein, J. L. R. (2008). *Dlx* genes pattern mammalian jaw primordium by regulating both lower jaw-specific and upper jaw-specific genetic programs. *Development* **135**, 2905-2916.
- Komori, T., Yagi, H., Nomura, S., Yamaguchi, A., Sasaki, K., Deguchi, K., Shimizu, Y., Bronson, R. T., Gao, Y. H., Inada, M. et al. (1997). Targeted disruption of *Cbfa1* results in a complete lack of bone formation owing to maturational arrest of osteoblasts. *Cell* **15**, 367-371.
- Kontges, G. and Lumsden, A. (1996). Rhombencephalic neural crest segmentation is preserved throughout craniofacial ontogeny. *Development* **122**, 3229-3242.

- Le Douarin, N. M. (1982). *The Neural Crest*. New York: Cambridge University Press.
- Lin, C. R., Kioussi, C., O'Connor, S., Briata, P., Szeto, D., Liu, F., Izpisua Belmonte, J. C. and Rosenfeld, M. G. (1999). Pitx2 regulates lung asymmetry, cardiac positioning and pituitary and tooth morphogenesis. *Nature* **401**, 279-282.
- Liu, W., Selever, J., Lu, M.-F. and Martin, J. F. (2003). Genetic dissection of *Pitx2* in craniofacial development uncovers new functions in branchial arch morphogenesis, late aspects of tooth morphogenesis and cell migration. *Development* **130**, 6375-6385.
- Maemura, K., Kurihara, H., Kurihara, Y., Oda, H., Ishikawa, T., Copeland, N. G., Gilbert, D. J., Jenkins, N. A. and Yazaki, Y. (1996). Sequence analysis, chromosomal location, and developmental expression of the mouse preproendothelin-1 gene. *Genomics* **31**, 177-184.
- McFadden, D. G., McAnally, J., Richardson, J. A., Charité, J. and Olson, E. N. (2002). Misexpression of dHAND induces ectopic digits in the developing limb bud in the absence of direct DNA binding. *Development* **129**, 3077-3088.
- McLellan, A. S., Kealey, T. and Langlands, K. (2006). An E box in the exon 1 promoter regulates insulin-like growth factor-I expression in differentiating muscle cells. *Am. J. Physiol. Cell Physiol.* **291**, 300-307.
- Miller, C. T., Schilling, T. F., Lee, K.-H., Parker, J. and Kimmel, C. B. (2000). *sucker* encodes a zebrafish Endothelin-1 required for ventral pharyngeal arch development. *Development* **127**, 3815-3838.
- Miller, C. T., Yelon, D., Stainier, D. Y. and Kimmel, C. B. (2003). Two endothelin 1 effectors, *hand2* and *bapx1*, pattern ventral pharyngeal cartilage and the jaw joint. *Development* **130**, 1353-1365.
- Mitsiadis, T. A. and Drouin, J. (2008). Deletion of the *Pitx1* genomic locus affects mandibular tooth morphogenesis and expression of the *Barx1* and *Tbx1* genes. *Dev. Biol.* **313**, 887-896.
- Miyama, K., Yamada, G., Yamamoto, T. S., Takagi, C., Miyado, K. and Sakai, M. (1999). A BMP-inducible gene, *Dlx5*, regulates osteoblast differentiation and mesoderm induction. *Dev. Biol.* **208**, 123-133.
- Morikawa, Y., D'Autreaux, F., Gershon, M. D. and Cserjesi, P. (2007). *Hand2* determines the noradrenergic phenotype in the mouse sympathetic nervous system. *Dev. Biol.* **307**, 114-126.
- Noden, D. M. and Francis-West, P. (2006). Differentiation and morphogenesis of craniofacial muscles. *Dev. Dyn.* **235**, 1194-1218.
- Otto, F., Thornell, A. P., Crompton, T., Denzel, A., Gilmour, K. C., Rosewell, I. R., Stamp, G. W., Beddington, R. S., Mundlos, S., Olsen, B. R. et al. (1997). *Cbfa1*, a candidate gene for cleidocranial dysplasia syndrome, is essential for osteoblast differentiation and bone development. *Cell* **89**, 765-771.
- Ozeki, H., Kurihara, Y., Tonami, K., Watatani, S. and Kurihara, H. (2004). Endothelin-1 regulates the dorsoventral branchial arch patterning in mice. *Mech. Dev.* **121**, 387-395.
- Rinon, A., Lazar, S., Marshall, H., Buchmann-Meller, S., Neufeld, A., Elhanany-Tamir, H., Taketo, M. M., Sommer, L., Krumlauf, R. and Tzahor, E. (2007). Cranial neural crest cells regulate head muscle patterning and differentiation during vertebrate embryogenesis. *Development* **134**, 3065-3075.
- Rivera-Perez, J. A., Mallo, M., Gendron-Maguire, M., Gridley, T. and Behringer, R. R. (1995). *gooseoid* is not an essential component of the mouse gastrula organizer but is required for craniofacial and rib development. *Development* **121**, 3005-3012.
- Ruest, L. B. and Clouthier, D. E. (2009). Elucidating timing and function of endothelin-A receptor signaling during craniofacial development using neural crest cell-specific gene deletion and receptor antagonism. *Dev. Biol.* **328**, 94-108.
- Ruest, L.-B., Dager, M., Yanagisawa, H., Charité, J., Hammer, R. E., Olson, E. N., Yanagisawa, M. and Clouthier, D. E. (2003a). *dHAND*-Cre transgenic mice reveal specific potential functions of dHAND during craniofacial development. *Dev. Biol.* **257**, 263-277.
- Ruest, L.-B., Hammer, R. E., Yanagisawa, M. and Clouthier, D. E. (2003b). *Dlx5/6*-enhancer directed expression of Cre recombinase in the pharyngeal arches and brain. *Genesis* **37**, 188-194.
- Ruest, L. B., Xiang, X., Lim, K. C., Levi, G. and Clouthier, D. E. (2004). Endothelin-A receptor-dependent and -independent signaling pathways in establishing mandibular identity. *Development* **131**, 4413-4423.
- Soriano, P. (1999). Generalized *lacZ* expression with the ROSA26 Cre reporter strain. *Nat. Genet.* **21**, 70-71.
- Talbot, J. C., Johnson, S. L. and Kimmel, C. B. (2010). *hand2* and *Dlx* genes specify dorsal, intermediate and ventral domains within zebrafish pharyngeal arches. *Development* **137**, 2507-2517.
- Thirumangalathu, S., Harlow, D. E., Driskell, A. L., Krimm, R. F. and Barlow, L. A. (2009). Fate mapping of mammalian embryonic taste bud progenitors. *Development* **136**, 1519-1528.
- Thomas, T., Kurihara, H., Yamagishi, H., Kurihara, Y., Yazaki, Y., Olson, E. N. and Srivastava, D. (1998). A signaling cascade involving endothelin-1, dHAND and *Mx1* regulates development of neural-crest-derived branchial arch mesenchyme. *Development* **125**, 3005-3014.
- Xiong, W., He, F., Morikawa, Y., Yu, X., Zhang, Z., Lan, Y., Jiang, R., Cserjesi, P. and Chen, Y. (2009). *Hand2* is required in the epithelium for palatogenesis in mice. *Dev. Biol.* **330**, 131-141.
- Yamada, G., Mansouri, A., Torres, M., Stuart, E. T., Blum, M., Schultz, M., De Robertis, E. M. and Gruss, P. (1995). Targeted mutation of the murine *gooseoid* gene results in craniofacial defects and neonatal death. *Development* **121**, 2917-2922.
- Yamagishi, H., Olson, E. N. and Srivastava, D. (2000). The basic helix-loop-helix transcription factor, dHAND, is required for vascular development. *J. Clin. Invest.* **105**, 261-270.
- Yanagisawa, H., Yanagisawa, M., Kapur, R. P., Richardson, J. A., Williams, S. C., Clouthier, D. E., de Wit, D., Emoto, N. and Hammer, R. E. (1998). Dual genetic pathways of endothelin-mediated intercellular signaling revealed by targeted disruption of endothelin converting enzyme-1 gene. *Development* **125**, 825-836.
- Yanagisawa, H., Clouthier, D. E., Richardson, J. A., Charité, J. and Olson, E. N. (2003). Targeted deletion of a branchial arch-specific enhancer reveals a role of dHAND in craniofacial development. *Development* **130**, 1069-1078.
- Zerucha, T., Stuhmer, T., Hatch, G., Park, B. K., Long, Q., Yu, G., Gambarotta, A., Schultz, J. R., Rubenstein, J. L. R. and Ekker, M. (2000). A highly conserved enhancer in the *Dlx5/Dlx6* intergenic region is the site of cross-regulatory interactions between *Dlx* genes in the embryonic forebrain. *J. Neurosci.* **20**, 709-721.